Proceedings of the 2nd Croatian Conference on Earthquake Engineering - 2CroCEE
Zagreb, Croatia - March 22 to 24, 2023

DOI: https://doi.org/10.5592/CO/2CroCEE.2023.12

NUMERICAL STUDY ON MECHANICAL PARAMETERS OF NOVEL DRILLED PLATE METALLIC DAMPER (DPMD)

Peyman Shadman Heidari [(1)]

[(1)] *Department of Civil Engineering, East Tehran Branch, Islamic Azad University, Tehran, Iran, peyman_shademan@yahoo.com*

Abstract

The purpose of this study is to investigate the seismic performance of a new type of yield metal dampers. Drilled plates are used in these metal dampers. These plates use holes with different diameters. Various drilling arrangement have also used to evaluate and improve the seismic performance of these types of dampers. For this study used a reference sample and 15 proposed models. The overall numerical results show that the proposed metal dampers have similar hysteretic curves. According to the hysteresis curves of drilled plate metallic damper (DPMD) under in-plane seismic loading; obtained mechanical parameters such as ductility ratio, initial stiffness, effective stiffness, total dissipated energy, dissipated energy in the last cycle, elastic strain energy, equivalent viscous damping (EVD) and equivalent plastic strain (EPS). Also, a formula is proposed to estimate the EVD value based on the ductility ratio of the proposed samples. The analytical results showed that the amount of stiffness, ductility ratio and equivalent viscous damping depends on the location and diameter of the holes. Also, the concentration of plastic strain between the holes increases the ductility ratio and EVD value of these types of dampers.

Keywords: Drilled Plate Metallic Damper (DPMD), Mechanical parameters, Ductility ratio, Equivalent viscous damping

1. Introduction

The occurrence of devastating earthquakes can cause life and financial losses. Especially the devastating earthquakes that have occurred in recent years around the world emphasize require of a suitable and reliable solution to this natural phenomenon. The performance of metallic dampers based on nonlinear behavior of metals is one of the most effective mechanisms of damping and absorption of input energy to structures during earthquakes. Kelly et al [1] used the idea of metallic dampers to absorb earthquakes energy in the structure. They introduced several hysteretic energy absorption mechanisms in structures. Skinner et al [2, 3] proposed several yielding metal dampers, including torsion beam dampers, bending beam dampers, and U-shaped dampers. Kasai and Popov [4] presented yielding damper using steel plate and stiffener. They tested it and introduced the hysteresis curve. Bergman and Goel [5] proposed flexural yielding metallic dampers. They tested added damping and stiffness (ADAS) and Triangular-ADAS (TADAS) systems. In ADAS and TADAS dampers are used parallel X and V shaped steel plates, respectively. Whittaker et al [6] tested X-shaped metallic dampers as ADAS under cyclic load. Tsai et al [7], in order to fix the defects of the XADAS dampers, studied TADAS triangular steel plate dampers. Also, they developed a simple mathematical model for force-displacement, which was reasonably accurate compared to laboratory work. Dargush and Soong [8] conducted a more detailed study of the phenomenon of fatigue in low cycles based on the behavioral theories of TADAS dampers and developed their analytical models. Gang Li and Hongnan Li [9] presented a new idea for designing metallic damper. They tested dual functions metallic damper (DFMD) with quasi-static loading. Soni and Sanghvi [10] described a technique to find out combined stiffness of model equipped with ADAS damper. They proposed a mathematical model. Teruna et al [11] investigated four steel damper specimens with specific geometry. They obtained energy absorption capabilities, hysteresis loop and stiffness in specimens. Sahoo et al [12] investigated passive energy dissipation of steel plates in both flexure and shear yielding under cyclic loading.

DOI: https://doi.org/10.5592/CO/2CroCEE.2023.12

Their specimens consist of two flexure (end) plates of X-shape and a shear (web) plate of rectangular shape. Garivani et al [13] introduced a new type of flexural yielding metallic damper and they called comb-teeth damper (CTD). Their damper included number of teeth steel plates that absorb energy through in-plane flexural yielding. Ghaedi et al [14] introduced a new hysteretic metallic bar damper that they named bar damper (BD). BD included three simple steel plates and a number of solid bars which dissipate input energy due to vibration loads through flexural yielding.
This research aims to introduce a new type of shear yielding metallic damper. In this type of dampers are used the shear plate with hole. Forasmuch as in this idea it is easy to construct and perform samples in the structure, various dampers can be produced by changing the location and diameter of the holes. Based on the hysteresis curves of DPMD sample under in-plane cyclic load; mechanical parameters such as ductility ratio, initial stiffness, effective stiffness, total dissipated energy, dissipated energy in the last cycle, elastic strain energy, equivalent viscous damping (EVD) and equivalent plastic strain (EPS) are determined.

2. Drilled Plate Metallic Damper

2.1. Geometry of DPMD

ADAS dampers are usually used in steel bracing frames, as shown in Figure 1. The DPMD consists of a series of drilled steel plates. In this new type of damper can produce a variety of DPMD with changing location and diameter of the holes.

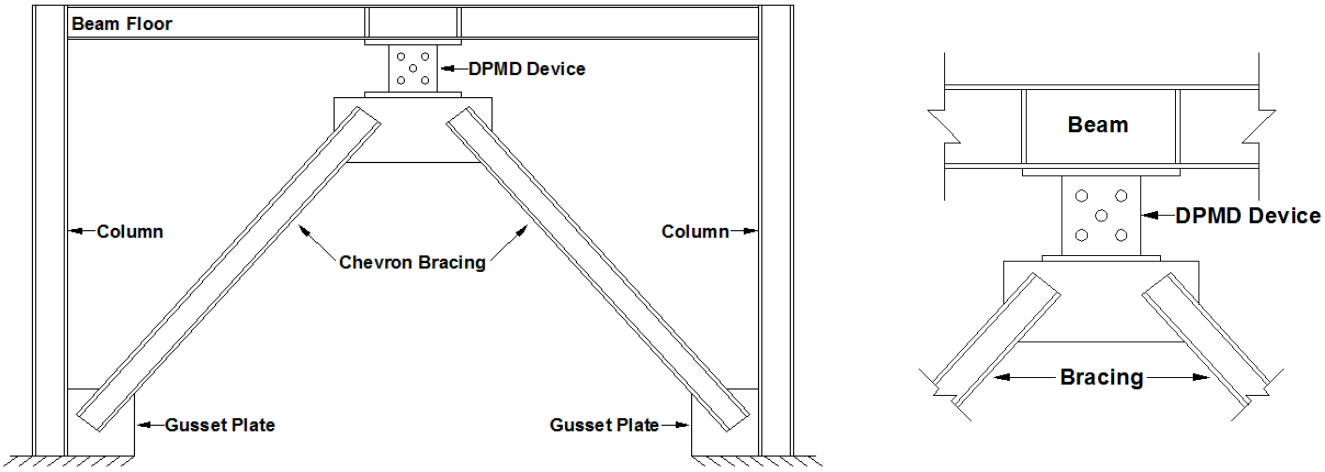

(a) (b)

Figure 1. a) Frame system and DPMD position, b) Connection of DPMD to beam and bracing

The 15 different models were proposed based on the various arrangements and diameter of the holes. All of samples have the same width, height and thickness 210, 300, 20 millimeters, respectively. Also thickness of end plate assumed 50 mm. In samples used diameter of holes 31.5, 42 and 52.5 mm which are equivalent to 30%, 40% and 50% reduction of cross sectional areas in plate, respectively. Figure 2 shows the drilling arrangement and the hole diameters of the samples.

DOI: https://doi.org/10.5592/CO/2CroCEE.2023.12

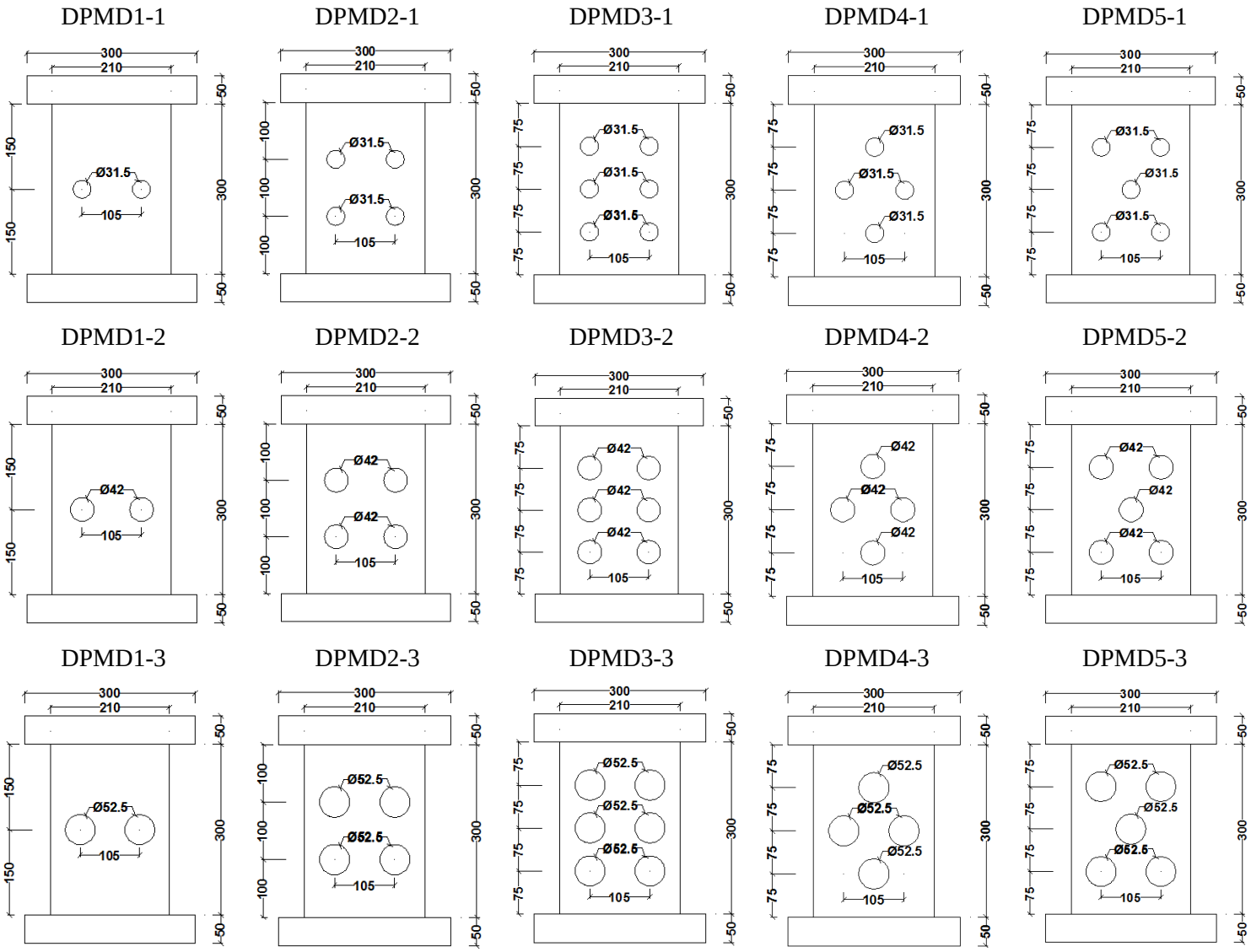

Figure 2. Details of samples

2.2.Loading pattern and material properties

In order to evaluate the performance of drilled plate metallic dampers; quasi-static cyclic loading pattern was used. Cyclic loading pattern specified by ATC 24 [15] was used for the cyclic loading of the analytical in this research. The loading pattern, magnitude of displacement and number of cycles are illustrated in Figure 3-a. There are seven steps with three cycles and other steps with two cycles. Displacement amplitude is from 1 to 84 mm. This general loading protocol is common for metallic damper. In this research mild steel plate was used with specifications that conform to JIS-SS400 [11]. The amount of yield stress, tensile strength and modulus of elasticity are 292, 456 and 2.06×10^{5} MPa respectively. Also, the measured yield strain and elongation are 1.42×10^{-3} and 16% respectively. Figure 3-b shows material strength curve [11].

Proceedings of the 2nd Croatian Conference on Earthquake Engineering - 2CroCEE
Zagreb, Croatia - March 22 to 24, 2023

DOI: https://doi.org/10.5592/CO/2CroCEE.2023.12

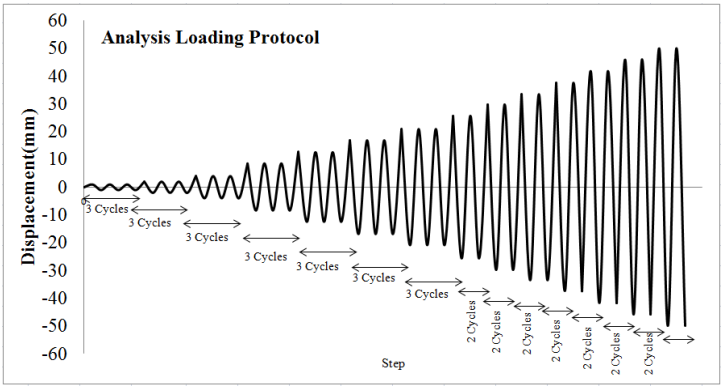

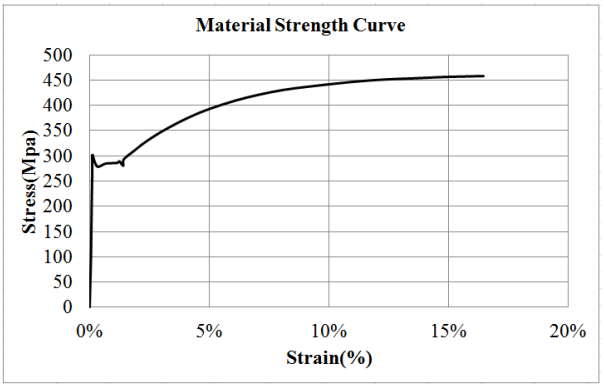

(a) (b)

Figure 3. a) The applied cyclic displacement loading protocol based on ATC-24[15], b) Stress-strain curve obtained from a coupon test [11]

3. Finite Element Modeling procedure

3.1.FEMs of DPMD

To study the mechanical parameters of the drilled plate metallic damper, nonlinear finite element (FE) analyses were carried out using ANSYS R16 FEM [16] software. Fifteen FEMs with different configurations and diameters were modeled. Steel plate elements were modeled using a 3D solid element. SOLID 185 (brick 8 node 185) element was used for modeling of proposed samples. Multi linear kinematic hardening plastic model [16] was used to model the plasticity and cyclic inelastic behavior of steel material, respectively. In order to prevent out of plane buckling of the end plate, the transitional degree of freedom in the Z and Y directions are closed. Mesh sensitivity analysis was performed to find proper element sizes in the FEMs. Mesh size was used 10x10 mm, and they are the same in all FEMs. Figure 4 shows the FEMs of the DPMD1-1, DPMD2-1, DPMD3-1, DPMD4-1 and DPMD5-1 used in this study.

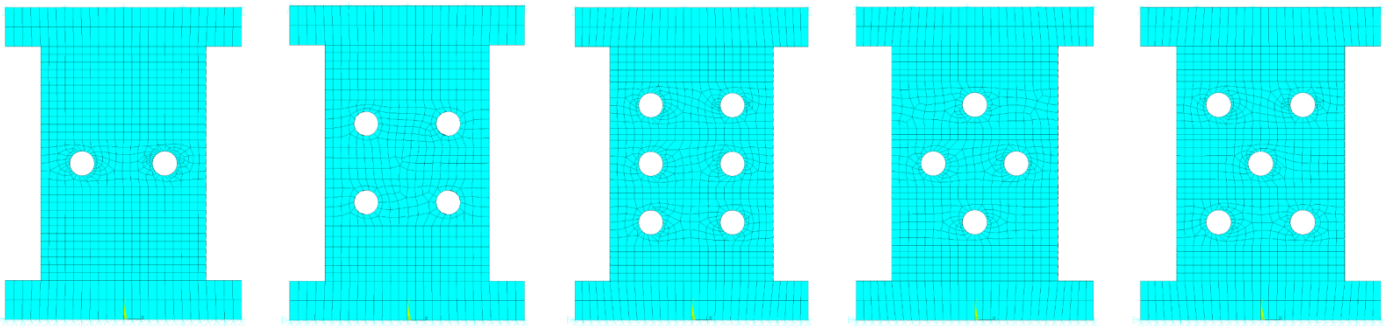

DPMD1-1 DPMD2-1 DPMD3-1 DPMD4-1 DPMD5-1

Figure 4. Finite element models of DPMD samples

3.2.FEM of DHSD-1 experimental specimen

In order to validate the FEMs, the experimental specimen (DHSD-1[11]) was modeled in ANSYS R16 FEM [16] software. Maximum displacement applied at top sample is 50.1 mm. Figure 5 illustrates details of test specimen, specimen shape and FEM in ANSYS software.

Proceedings of the 2nd Croatian Conference on Earthquake Engineering - 2CroCEE
Zagreb, Croatia - March 22 to 24, 2023

DOI: https://doi.org/10.5592/CO/2CroCEE.2023.12

(a): Details of test specimen [11] (b): Specimen shape [11] (c): FEM

Figure 5. Experimental and Finite element models [11]

The results of analytical and experimental analysis were compared. According to Figure 6, there is an acceptable agreement between the results of analytical and experimental studies.

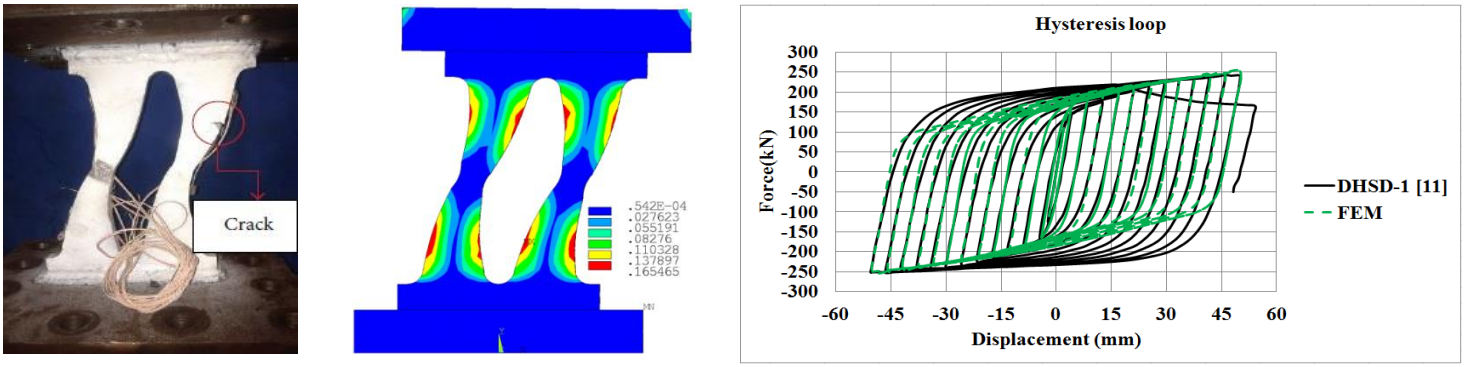

(a): Failure of specimen [11] (b): Total mechanical strain (c): Hysteresis curve of experimental and FEM of DHSD-1[11]

Figure 6. Failure of specimen, distribution of Total mechanical strain at maximum displacement and Comparison of hysteresis curves

3.3.Hysteresis behavior of DPMDs

Hysteresis curves are needed to determine the mechanical parameters of the DPMD proposed damper. In the force-displacement hysteresis curve such as yield force, yield displacement, ultimate force, and ultimate displacement can be obtained parameters. For this purpose, force-displacement hysteresis curves of analytical samples were determined. Figure 7 shows the force-displacement hysteresis curves of the DPMD dampers.

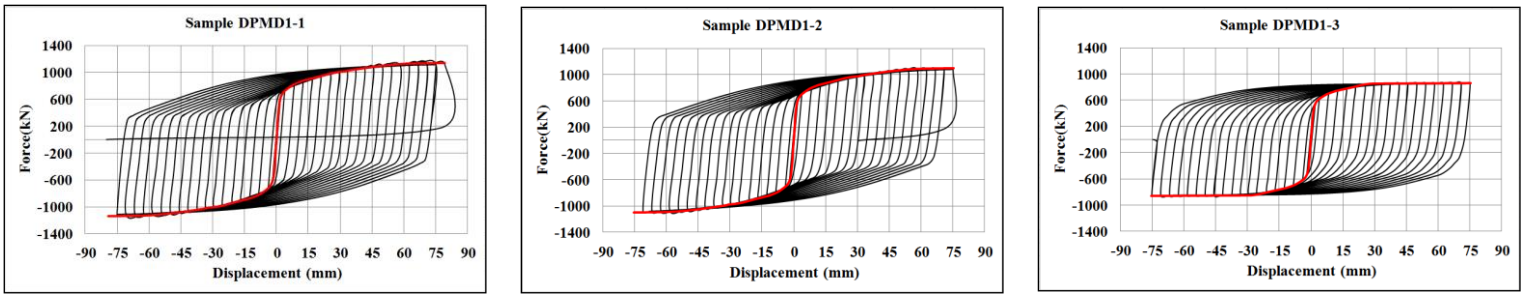

Proceedings of the 2nd Croatian Conference on Earthquake Engineering - 2CroCEE
Zagreb, Croatia - March 22 to 24, 2023

DOI: https://doi.org/10.5592/CO/2CroCEE.2023.12

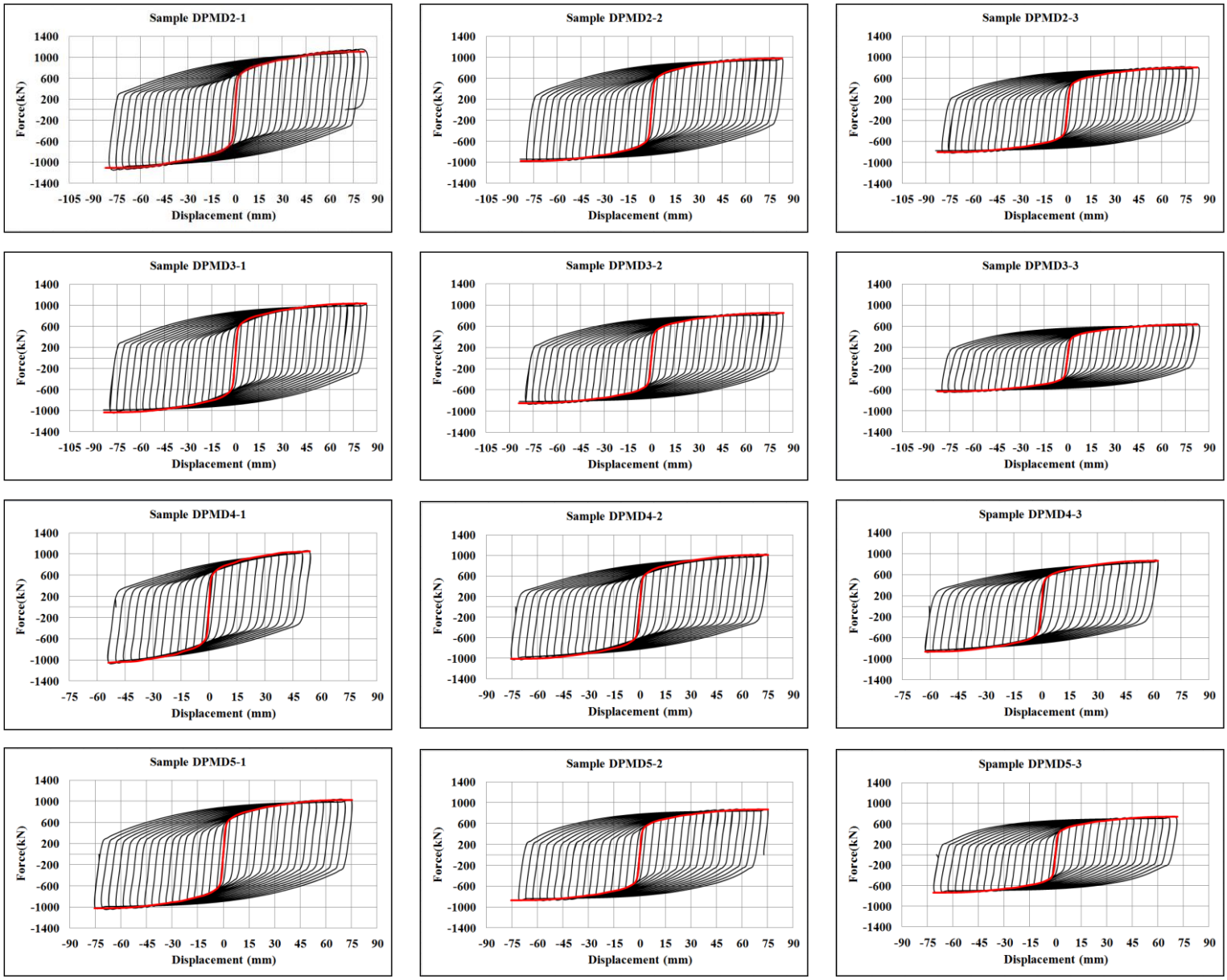

Figure 7. Force-displacement hysteresis loops of the DPMD and backbone curves

4. Mechanical parameters of DPMD dampers

4.1.Ductility ratio, effective and initial stiffness, total dissipated energy and equivalent viscous damping

Ductility ratio can be defined as the ratio of maximum deformation capacity to the deformation level corresponding to a yield deformation. The value of ductility ratio is given by:

$$\mu = \frac{\Delta_{\max}}{\Delta_y} \tag{1}$$

Where $\Delta_{\max}$ and Δ_y are ultimate displacement and yield displacement, respectively. In each loop of the force-deformation hysteresis curve the secant or effective stiffness can be defined. The effective stiffness for maximum displacement was obtained as the average from minimum and maximum force

Proceedings of the 2nd Croatian Conference on Earthquake Engineering - 2CroCEE
Zagreb, Croatia - March 22 to 24, 2023

DOI: https://doi.org/10.5592/CO/2CroCEE.2023.12

over the average from minimum and maximum displacement, respectively. According to Figure 8, effective stiffness equation is obtained as follows:

$$K_{eff} = \frac{\frac{|P_{max}| + |P_{min}|}{2}}{\frac{|\Delta_{max}| + |\Delta_{min}|}{2}} = \frac{P_{ave}}{\Delta_{ave}} \tag{2}$$

Where Δ_{max}, Δ_{min}, Δ_{ave}, P_{max}, P_{min} and P_{ave} are ultimate displacement, minimum displacement, average displacement, ultimate force, minimum force, average force in each loop, respectively. In this research, effective stiffness was calculated for maximum displacement and last loop of the force-displacement hysteresis curves of the DPMD samples. Also, initial stiffness is calculated as follows:

$$K_{initial} = \frac{P_y}{\Delta_y} \tag{3}$$

Where Δ_y and P_y are yield displacement and yield force, respectively. In this paper, initial stiffness was calculated for first loop of the force-displacement hysteresis curves of the DPMD samples. Effective stiffness represents the damping force in response to the desired displacement. The ultimate displacement and yield displacement values were obtained from the force-displacement hysteresis curve. Table 1 illustrates the ductility ratio, effective stiffness and initial stiffness for the DPMD samples.

The rate of damage in structures under seismic load depends on transfer seismic energy. By using passive dampers a large amount of seismic energy can be absorbed. Therefore, the amount of seismic energy absorbed by the principal structural members is reduced, and structure elements have elastic behavior. The amount of energy absorption per cycle is the area under the force-displacement hysteresis curve for one loop. Figure 8 shows amount of energy dissipated in last cycle and elastic strain energy. The amount of total dissipated energy in each force-displacement hysteresis curve includes the sum of the areas under the curve of all cycles. In this study, E_T, E_D and E_S are total dissipated energy, dissipated energy in the last cycle and elastic strain energy, respectively. According to the description given and existing hysteresis curves, it is possible to calculate total dissipated energy, dissipated energy in the last cycle and elastic strain energy. The E_T, E_D and E_S values are shown in Table 2.

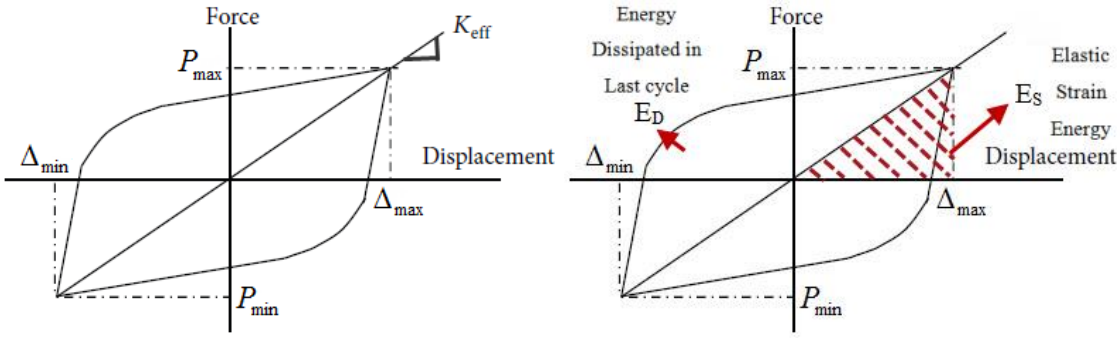

Figure 8. Definition of effective stiffness and energy dissipated in the last cycle and elastic strain energy

Proceedings of the 2nd Croatian Conference on Earthquake Engineering - 2CroCEE
Zagreb, Croatia - March 22 to 24, 2023

DOI: https://doi.org/10.5592/CO/2CroCEE.2023.12

Table 1 – Ductility ratio, effective stiffness and initial stiffness of DPMD samples

Series	**FEMs Pattern**	Δ_y **(mm)**	Δ_{max} **(mm)**	Δ_{min} **(mm)**	Δ_{ave} **(mm)**	P_y **(kN)**	P_{max} **(kN)**	P_{min} **(kN)**	P_{ave} **(kN)**	μ	$K_{initial}$ **(kN/mm)**	K_{eff} **(kN/mm)**
DPMD1	DPMD1-1	1.75	75.1	-74.4	74.8	603	1112	-1113	1113	42.91	344.6	14.883
	DPMD1-2	1.67	70.9	-70.9	70.9	585	1077	-1078	1078	42.46	350.3	15.197
	DPMD1-3	1.66	75.2	-75.2	75.2	513	850	-850	850	45.30	309.0	11.303
DPMD2	DPMD2-1	1.84	79.2	-79.3	79.3	579	1087	-1087	1087	43.04	314.7	13.716
	DPMD2-2	1.82	83.6	-79.4	81.5	519	939	-938	939	45.93	285.2	11.515
	DPMD2-3	1.81	83.6	-79.4	81.5	428	774	-774	774	46.19	236.5	9.497
DPMD3	DPMD3-1	1.86	83.5	-79.3	81.4	549	988	-987	988	44.89	295.2	12.131
	DPMD3-2	1.84	83.6	-79.4	81.5	452	813	-812	813	45.43	245.7	9.969
	DPMD3-3	1.83	83.7	-79.5	81.6	338	608	-607	608	45.74	184.7	7.445
DPMD4	DPMD4-1	1.19	54.1	-54.1	54.1	543	1028	-1028	1028	45.46	456.3	19.002
	DPMD4-2	1.65	75.1	-75.1	75.1	537	984	-984	984	45.52	325.5	13.103
	DPMD4-3	1.38	62.6	-62.6	62.6	458	839	-839	839	45.36	331.9	13.403
DPMD5	DPMD5-1	1.68	75.1	-75.1	75.1	543	987	-987	987	44.70	323.2	13.142
	DPMD5-2	1.64	71.0	-71.0	71.0	464	841	-841	841	43.29	282.9	11.845
	DPMD5-3	1.58	71.1	-71.1	71.1	392	699	-699	699	45.00	248.1	9.831

The highest and lowest ductility values are for DPMD2-3 and DPMD1-2 samples, respectively. As can be seen, the proposed samples have high ductility values. Due to the high ductility of the proposed samples, it is possible to tolerate non-elastic deformations without significant degradation of strength and stiffness in the structures.

The equivalent viscous damping (EVD) or effective damping is effective index in evaluating the seismic performance of passive energy dissipation systems. The EVD has defined the combined effects of elastic and hysteretic damping. The EVD concept was first proposed by Jacobsen [17, 18]. The value of EVD based on Jacobsen's approach can be calculated with equation 4. The ξ_{hyst} represents the dissipation energy due to the hysteretic behavior.

$$\xi_{hyst} = \frac{E_D}{4\pi E_S} = \frac{E_D}{2\pi K_{eff}\delta_{ave}^{\ 2}} \tag{4}$$

Table 2 presents equivalent viscous damping for the fifteen samples of DPMD. It is calculated at the maximum displacement. The EVD of DPMPs can be calculated using the proposed formula below.

$$\xi_{equ} = 0.055\mu^{0.58} \tag{5}$$

Proceedings of the 2nd Croatian Conference on Earthquake Engineering - 2CroCEE
Zagreb, Croatia - March 22 to 24, 2023

DOI: https://doi.org/10.5592/CO/2CroCEE.2023.12

The calculated error values can also be computed as follows:

$$\%e = \frac{\xi_{equ} - \xi_{hyst}}{\xi_{hyst}} \times 100 \tag{6}$$

Also, Table 2 shows the values of ξ_{equ} and error values of proposed formula with Jacobsen's approach.

Table 2 – Total dissipated energy, dissipated energy in the last cycle, elastic strain energy and EVD of DPMD samples and proposed formula

Series	**FEMs Pattern**	E_T **(N.m)**	E_D **(N.m)**	E_S **(N.m)**	$\frac{E_D}{E_T}$	$\frac{E_S}{E_T}$	EVD $\xi_{hyst}(\%)$	**Proposed formula** $\xi_{equ}(\%)$	**%e**
DPMD1	DPMD1-1	4546533.1	300509.2	41579.7	6.6%	0.9%	57.5	48.67	-15.4
	DPMD1-2	3895810.1	228666.5	38197.4	5.9%	1.0%	47.6	48.37	1.5
	DPMD1-3	3938765.4	222333.9	31960.0	5.6%	0.8%	55.4	50.22	-9.3
DPMD2	DPMD2-1	4840810.6	258172.2	43072.4	5.3%	0.9%	47.7	48.76	2.2
	DPMD2-2	4508396.9	241985.7	38243.9	5.4%	0.8%	50.4	50.63	0.5
	DPMD2-3	3838292.5	210534.2	31540.5	5.5%	0.8%	53.1	50.79	-4.4
DPMD3	DPMD3-1	4662833.4	259236.2	40191.3	5.6%	0.9%	51.3	49.96	-2.7
	DPMD3-2	3957426.1	219552.2	33109.4	5.5%	0.8%	52.8	50.31	-4.7
	DPMD3-3	3029986.1	164074.1	24786.0	5.4%	0.8%	52.7	50.50	-4.1
DPMD4	DPMD4-1	2104193.4	160074.9	27807.4	7.6%	1.3%	45.8	50.33	9.9
	DPMD4-2	3835282.4	219018.9	36949.2	5.7%	1.0%	47.2	50.36	6.8
	DPMD4-3	2360628.2	156908.4	26260.7	6.6%	1.1%	47.5	50.26	5.7
DPMD5	DPMD5-1	4047102.7	233607.3	37061.9	5.8%	0.9%	50.2	49.84	-0.6
	DPMD5-2	3309210.9	194731.8	29855.5	5.9%	0.9%	51.9	48.92	-5.8
	DPMD5-3	2706086.6	163682.2	24849.5	6.0%	0.9%	52.4	50.03	-4.6

Due to the maximum displacement value of 79.3 mm and maximum force value of 1087 kN, the most total energy absorption occurred in DPMD2-1 sample. On the other hand, the total energy absorption of the samples decreases by increasing the amount of cross-sectional area reduction from 30% to 50% in the series samples. Also, elastic strain energy decreases by increasing the cross-section reduction in the series samples. The almost in all series increased the EVD amount with increasing cross-sectional area reduction. DPMD1-1 sample have most of equivalent viscous damping. Increasing the amount of damping ratio ξ increases the damping in the structural system. On the other hand, increasing damping in structure causes decreases response spectra under severe seismic load.

4.2. Equivalent plastic strain

The equivalent plastic strain (EPS) is calculated from the component plastic strain. The equivalent plastic strain is a scalar parameter that ANSYS output label is EPEQ. The EPS describes the degree of

Proceedings of the 2nd Croatian Conference on Earthquake Engineering - 2CroCEE
Zagreb, Croatia - March 22 to 24, 2023

DOI: https://doi.org/10.5592/CO/2CroCEE.2023.12

work hardening in a material. Increasing the equivalent plastic strain increases the fracture potential. Reduction of equivalent plastic strain indicates a decrease in strain as well as an increase in the ductility of the material. The EPS inappropriate distribution causes stress concentration and rapid crack growth. The equivalent plastic strain can be defined as follows:

$$EPS = \varepsilon_{eqv}^{pl} = \sqrt{\frac{2}{3}\varepsilon_{ij}^{pl}\varepsilon_{ji}^{pl}} \tag{7}$$

Where ε_{ij}^{pl} and ε_{ji}^{pl} are components of plastic strain. Figure 9 illustrates distribution of equivalent plastic strain in maximum displacement of DPMD samples. Also, in figure 10 comparison of the maximum equivalent plastic strain of DPMD samples is shown.

DPMD1-1 DPMD2-1 DPMD3-1 DPMD4-1 DPMD5-1

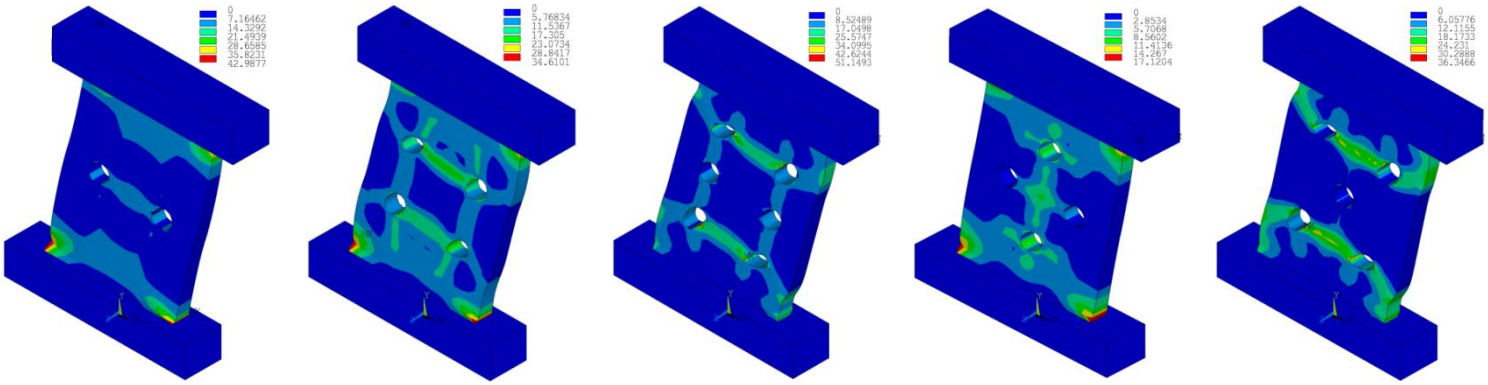

DPMD1-2 DPMD2-2 DPMD3-2 DPMD4-2 DPMD5-2

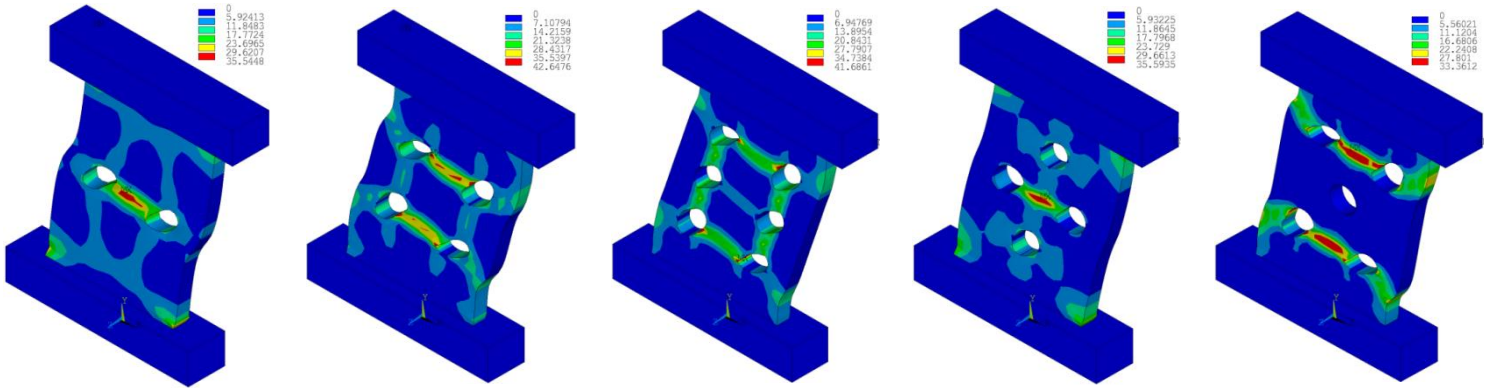

DPMD1-3 DPMD2-3 DPMD3-3 DPMD4-3 DPMD5-3

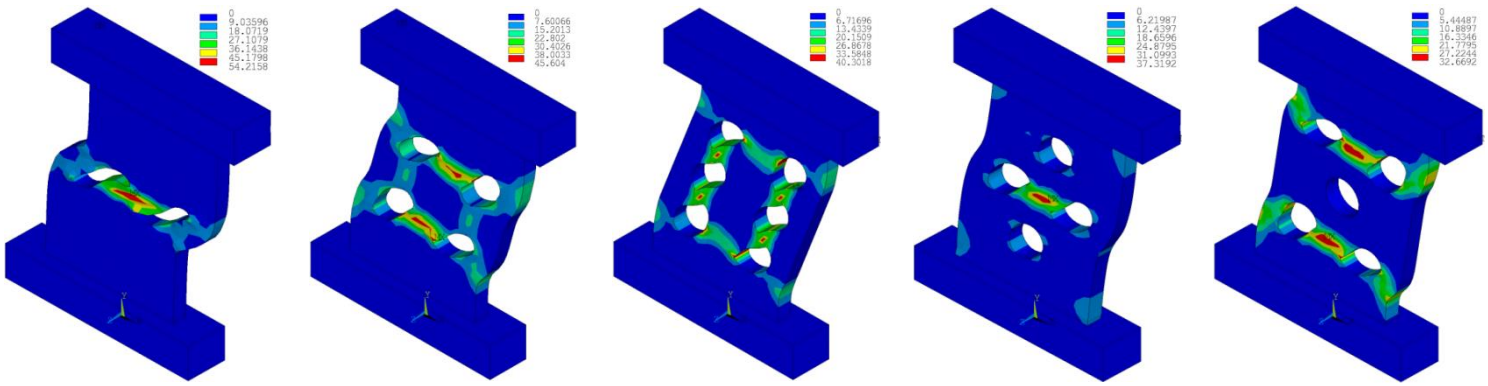

DOI: https://doi.org/10.5592/CO/2CroCEE.2023.12

Figure 9. Distribution of equivalent plastic strain in maximum displacement of DPMD samples

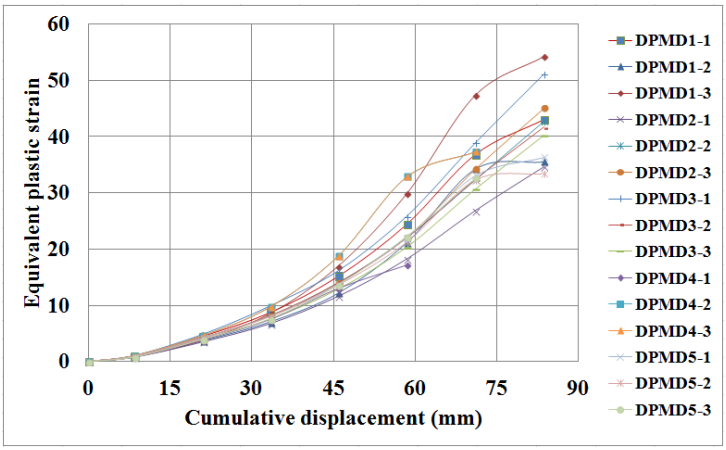

Figure 10. Comparison of the maximum equivalent plastic strain of DPMD samples in each displacement

$$MEPS(\Delta) = -0.104\Delta^4 + 1.529\Delta^3 - 6.639\Delta^2 + 14.307\Delta - 8.3 \quad (8)$$

Where $MEPS(\Delta)$ and Δ are the maximum equivalent plastic strain and applied displacement top of sample, respectively. In all the proposed samples, with changing the location of the holes changes the distribution of equivalent strain. The contour plots show that the plastic strain and failures started to grow from corners of shear plate and beside the holes. In each series of samples proposed, with increasing cross section reduction changes the location of occurrence of the maximum equivalent plastic strain. The location of the maximum equivalent plastic strain changes from the corners of the shear plate to the intermediate between the holes. The lowest amount of EPS occurs in the DPMD2-1 sample.

5. Conclusions

In this study, a new shear yielding metallic damper is introduced. The advantage of this type of damper is simple implementation procedure using the drilling of the plate. Changing the drilling arrangement and the diameter of the holes are effective on the mechanical parameters of the dampers. By studying the finite element analysis of the proposed samples, it is observed that the ductility ratio and EVD can be increased by increasing the diameter of the holes. Total dissipated energy, dissipated energy in the last cycle, elastic strain energy, initial stiffness and effective stiffness decrease as the increasing diameter of the holes. The DPMD2-3 sample has a ductility ratio of 46.19 which is the maximum amount among the other samples. Also, the maximum EVD occurs in DPMD1-1 sample. The maximum error between the values of EVD based on Jacobsen's approach and the values of EVD based on proposed formula is less than 15.4%. In most cases the EVD of proposed formula values have good accuracy. The location and increasing the diameter of the holes can be effective in changing the location of the start rupture from the corner of the shear plate to beside of the holes. Given the amount of maximum EPS and contour plot, the start location and growth of crack in samples with high EVD than others begins near the holes.

6. Acknowledgment

We would like to thank Department of Civil Engineering, East Tehran Branch, Islamic Azad University for finical support of this paper.

Proceedings of the 2nd Croatian Conference on Earthquake Engineering - 2CroCEE
Zagreb, Croatia - March 22 to 24, 2023

DOI: https://doi.org/10.5592/CO/2CroCEE.2023.12

7. References

[1] Kelly J.M., Skinner R.1., Heine A.J., (1972): Mechanisms of Energy Absorption in Special Devices for Use in Earthquake Resistant Structures. *Bulletin of N. Z. Society of Earthquake Engineering*, Vol. 5 No. 3.

[2] Skinner R.1., Kelly J.M., Heine A.J., (1975): Hysteretic Dampers for Earthquake Resistant Structures. *Earthquake Engineering and Structural Dynamics*, 287- 296.

[3] Skinner R.1., Tyler R.G., Heine A.J. and Robinson W.H., (1980): Hysteretic Dampers for the Protection of Structures from Earthquakes. *Bulletin of N. Z. Society of Earthquake Engineering*, Vol 13. No 1.

[4] Kasai K., Popov E.P., (1986): General behavior of WF steel shear link beams. *J. Struc. Eng.*, 112(2), 362-382.

[5] Bergman D. M., Goel S.C., (1987): Evaluation of cyclic testing of steel plate device for added damping and stiffness. *Report No. UMCE 87-10, the University of Michigan, Ann Arbor, MI.*

[6] Whittaker A.S., Bertero V.V., Thompson C. L., Alonso L.J., (1991): Seismic Testing of Steel Plate Energy Dissipation Devices. *Earthquake Spectr*, Vol. 7, No. 4, pp. 563-604.

[7] Tsai K.C., Chen H.W., Hong C.P., Su Y.F., (1993): Design of steel triangular plate energy absorbers for seismic-resistance construction. *Earthquake Spectra*, 9(3), pp. 505-528.

[8] Dargush G.F., Soong T.T., (1995): Behavior of Metallic Plate Dampers in Seismic Passive Energy Dissipation Systems. *Earthquake Spectra*, 11(4), 545-568.

[9] Gang Li, Hongnan Li, (2008): Earthquake resistant design of RC frame with dual functions metallic damper. *The 14th World Conference on Earthquake Engineering.* Beijing, China.

[10] Soni A.H., Sanghvi C.S., (2012): Mathematical modeling of ADAS damper element and nonlinear time history analysis of SDOF steel structure using ETABS. *Journal of Engineering Research and Studies.*

[11] Teruna D.R., Majid T.A., Budiono B.,(2015): Experimental Study of Hysteretic Steel Damper for Energy Dissipation Capacity. *Advances in Civil Engineering*, Article ID 631726, 12 pages.

[12] Sahoo D.R, Singhal T., Taraithia S.S, Saini A., (2015): Cyclic behavior of shear-and-flexural yielding metallic dampers. *Journal of Constructional Steel Research*, 114 (2015) 247–257.

[13] Garivani S., Aghakouchak A.A., Shahbeyk S., (2016): Numerical and Experimental Study of Comb-Teeth Metallic Yielding Dampers. *International Journal of Steel Structures*, 16(1), 177-196.

[14] Ghaedi K., Ibrahim Z., javanmardi A., (2018): A new metallic bar damper device for seismic energy dissipation of civil structures. *14th International Conference on Concrete Engineering and Technology.*

[15] ATC 24., (1992): Guidelines for cyclic seismic testing of components of steel structures. *Applied Technology Council.*

[16] ANSYS Meshing User's Guide, (2016), Release 16.0. ANSYS, Inc.

[17] Jacobsen L.S., (1930): Steady forced vibration as influenced by damping. *Transactions of ASME*, 52, 169–181.

[18] Jacobsen L.S., (1960): Damping in composite structures, *Proceedings of the Second World Conference on Earthquake Engineering*, Vol 2, pp. 1029–1044.